Drawing Force in the Deep Drawing Utilizing Lateral Fluid Pressure

Drawing Force in the Deep Drawing Utilizing Lateral Fluid Pressure

Kenji ASAKURA*, Nobuo KOBAYASHI* and Masahide KOHZU*

(Received June 15, 1984)

The drawing characteristics in this deep drawing clarified experimentally in the previous paper have been studied theoretically by stress analysis. The theoretical equations of drawing force and punch pressure, in which bending and frictional effects were considered, were derived by the analysis based on the assumptions of axisymmetric deformation and plane strain. The theoretical values calculated by these equations agreed well with the experimental values. The drawing characteristics may be estimated theoretically for different working conditions by use of the equations.

1. Introduction

The authors have already clarified experimentally the drawing characteristics in this deep drawing for soft aluminum sheet[1], and have clarified the degrees of the contributions of punch pressure and lateral fluid pressure to the drawing deformation by unifying these pressures as the components of the drawing force in this deep drawing[2].

In this study, by the stress analysis based on the assumptions of axisymmetric deformation and plane strain, the theoretical equation of drawing force, in which bending and frictional effects are considered, are derived to estimate theoretically the drawing characteristics for different working conditions.

2. Theoretical Equation of the Drawing Force

As shown in the previous paper[2], the drawing force F in this deep drawing can be divided into two components, F_p due to punch pressure p_p and F_s due to lateral fluid pressure p_s, and is given by:

$$F = F_p + F_s = \pi r_p^2 \cdot p_p + 2\pi r_i t \cdot p_s \ , \tag{1}$$

where $r_i = (r_p + r_d) / 2$ (see Fig. 1). The value of F obtained by substituting the experimental values in Eq. (1) is named the experimental value of drawing force, and is distinguished from the theoretical value of F obtained by the stress analysis carried out in following sections.

The component F_p, which is punch force, and punch pressure p_p can be expressed as:

$$F_p = 2\pi r_i t \cdot \sigma_{ri} \tag{2}$$

$$p_p = \frac{2 r_i t}{r_p^2} \sigma_{ri} \ , \tag{3}$$

* Department of Metallurgical Engineering, College of Engineering.

where σ_{ri} is the normal stress produced on the cross section of cup wall by punch. Substituting Eq. (3) in Eq. (1),

$$F = 2\pi r_i t(\sigma_{ri} + p_s) \ . \tag{4}$$

In the analysis of the drawing force, the axisymmetric deformation and plane strain are assumed. In this deep drawing, a blank is ironed by the tapered surface of the protrusion of the hold-down cylinder as shown in Fig. 1[1]. But, in practice, the ironing is so light that its effect on the drawing force is unconsidered.

The dimensional symbols of tools and blank are shown in Fig. 1.

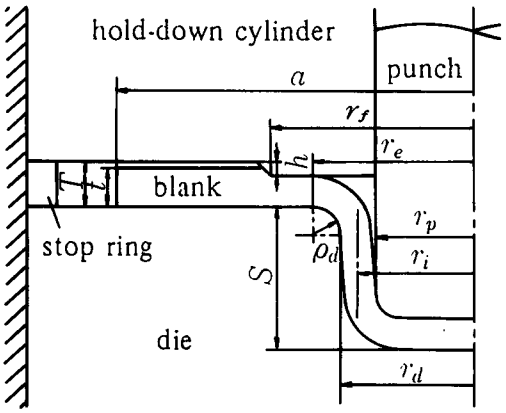

Fig. 1 Dimensional symbols of tools and blank

2.1 Analysis unincluding frictional effect

When a blank diameter changes from its initial value $2a_0$ to $2a$ by drawing the blank up to drawing depth S, the following equation is obtained from the assumptions of axisymmetric deformation and plane strain.

$$r_0^2 - r^2 = a_0^2 - a^2 = 2r_i S \ , \tag{5}$$

where r_0 and r are the initial and current radii to a particle in flange, respectively. The equivalent strain $\bar{\varepsilon}$ and equivalent stress $\bar{\sigma}$ become :

$$\bar{\varepsilon} = \frac{2}{\sqrt{3}} \ln \frac{r_0}{r} \ , \tag{6}$$

$$\bar{\sigma} = \frac{\sqrt{3}}{2}(\sigma_r - \sigma_\theta) \ , \tag{7}$$

where σ_r, and σ_θ are meridian and circumferential stresses, respectively. The relation between $\bar{\sigma}$ and $\bar{\varepsilon}$ is given by :

$$\bar{\sigma} = C\bar{\varepsilon}^n \ , \tag{8}$$

where C is work hardening factor and n is work hardening exponent.

Generally, the equilibrium equation of stress in flange is given by :

$$\frac{d\sigma_r}{dr}+\frac{\sigma_r-\sigma_\theta}{r}=0 \ . \tag{9}$$

Then, using Eqs. (5) ~ (8),

$$\frac{d\sigma_r}{dr}=C\left(\frac{2}{\sqrt{3}}\right)^{n+1}\frac{1}{r}\left(\ln\frac{\sqrt{2r_iS+r^2}}{r}\right)^n \ . \tag{10}$$

Then, integrating and using the boundary condition $\sigma_r=-p_S$ at the rim of flange ($r=a$), the stress acting at the cross section of cup wall, which can be identified with the stress acting at the idealized inner rim of flange ($r=r_i$), can be expressed as :

$$\sigma_{riF}=C\left(\frac{2}{\sqrt{3}}\right)^{n+1}\int_{ri}^{a}\frac{1}{r}\left(\ln\frac{\sqrt{2r_iS+r^2}}{r}\right)^n dr-p_S \ , \tag{11}$$

where a is given by $\sqrt{a_0{}^2-2r_iS}$ from Eq. (5), and the subscript F denotes that the frictional effect is unconsidered.

According to Siebel's equation, the stress required for bending and unbending, σ_G, can be written as:

$$\sigma_G=t(\bar{\sigma}_e+\bar{\sigma}_i)/4\rho \ , \tag{12}$$

where $\bar{\sigma}_e$ and $\bar{\sigma}_i$ are the equivalent stresses at $r=r_e$ and $r=r_i$, and ρ is $\rho_d+t/2$. Then, using Eqs. (6) and (8),

$$\sigma_G=\frac{Ct}{4\rho}\left\{\left(\frac{2}{\sqrt{3}}\ln\frac{\sqrt{2r_iS+r_e{}^2}}{r_e}\right)^n+\left(\frac{2}{\sqrt{3}}\ln\sqrt{\frac{2S}{r_i}+1}\right)^n\right\} \ . \tag{13}$$

Therefore, substituting the sum of σ_{riF} [Eq. (11)] and σ_G [Eq. (13)] for σ_{ri} in Eqs. (4) and (3), the drawing force F' and punch pressure p_p', in which the frictional effect is unconsidered, can be expressed as :

$$F'=2\pi r_it C\left(\frac{2}{\sqrt{3}}\right)^{n+1}\int_{r_i}^{a}\frac{1}{r}\left(\ln\frac{\sqrt{2r_iS+r^2}}{r}\right)^n dr$$
$$+\frac{\pi r_it^2C}{2\rho}\left\{\left(\frac{2}{\sqrt{3}}\ln\frac{\sqrt{2r_iS+r_e{}^2}}{r_e}\right)^n+\left(\frac{2}{\sqrt{3}}\ln\sqrt{\frac{2S}{r_i}+1}\right)^n\right\} \ , \tag{14}$$

$$p_p'=\frac{2r_it}{r_p{}^2}\left\{C\left(\frac{2}{\sqrt{3}}\right)^{n+1}\int_{r_i}^{a}\frac{1}{r}\left(\ln\frac{\sqrt{2r_iS+r^2}}{r}\right)^n dr-p_S\right\}$$
$$+\frac{r_it^2C}{2\rho r_p{}^2}\left\{\left(\frac{2}{\sqrt{3}}\ln\frac{\sqrt{2r_iS+r_e{}^2}}{r_e}\right)^n+\left(\frac{2}{\sqrt{3}}\ln\sqrt{\frac{2S}{r_i}+1}\right)^n\right\} \ . \tag{15}$$

2.2 Analysis including frictional effect

As described in the previous paper[1], in the outer region than the protrusion of hold-down cylinder($r>r_f$: see Fig. 1), lubricant (tallow) is kept between blank and tools, and the state of fluid lubrication persists throughout the drawing process. On the other hand, the region ($r_e< r < r_f$) at which the pressurized liquid is sealed is in the state of boundary lubrication. Therefore, the frictional effect is considered for only the later region in this analysis.

In this region, the thickness of blank is unchangeable because of the restraint by tools. Using Eq.(7), the thickness stress σ_t is given by:

$$\sigma_t = \frac{\sigma_r+\sigma_\theta}{2} = \sigma_r - \frac{\bar{\sigma}}{\sqrt{3}} \ . \tag{16}$$

Considering a small ring element at radius r in this region, the frictional force acting on its upper and lower surfaces is given by $-4\pi r dr\cdot\mu\sigma_t$. Using Eq. (16), the radial stress against this friction, $d\sigma_H$, which acts on the inner lateral surface of this element, is given by:

$$d\sigma_H = -\frac{2dr\cdot\mu\sigma_t}{t} = \frac{2\mu}{t}\left(\frac{\bar{\sigma}}{\sqrt{3}}-\sigma_r\right)dr \ . \tag{17}$$

$\bar{\sigma}$ can be expressed as the function of r by using Eqs. (5), (6) and (8) and also σ_r can be expressed as its function by replacing the lower limit r_i of the integral in Eq. (11) to r. Then, integrating this expression from r_e to r_f,

$$\sigma_H = \frac{2\mu}{t}\left\{\frac{C}{\sqrt{3}}\left(\frac{2}{\sqrt{3}}\right)^n\int_{r_e}^{r_f}\left(\ln\frac{\sqrt{2r_iS+r^2}}{r}\right)^n dr + p_s(r_f-r_e)\right.$$

$$\left. - C\left(\frac{2}{\sqrt{3}}\right)^{n+1}\int_{r_e}^{r_f}\int_r^a\frac{1}{r}\left(\ln\frac{\sqrt{2r_iS+r^2}}{r}\right)^n dr\cdot dr\right\} \ . \tag{18}$$

Therefore, substituting the sum of σ_{riF} [Eq. (11)], σ_G [Eq. (13)] and σ_H [Eq. (18)] for σ_{ri} in Eq. (4), the equation of drawing force F, in which the frictional effect is considered, can be expressed as:

$$F = 2\pi r_i t C\left(\frac{2}{\sqrt{3}}\right)^{n+1}\int_{r_i}^a\frac{1}{r}\left(\ln\frac{\sqrt{2r_iS+r^2}}{r}\right)^n dr$$

$$+\frac{\pi r_i t^2 C}{2\rho}\left\{\left(\frac{2}{\sqrt{3}}\ln\frac{\sqrt{2r_iS+r_e^2}}{r_e}\right)^n+\left(\frac{2}{\sqrt{3}}\ln\sqrt{\frac{2S}{r_i}+1}\right)^n\right\}$$

$$+4\pi r_i\mu\left\{\frac{C}{\sqrt{3}}\left(\frac{2}{\sqrt{3}}\right)^n\int_{r_e}^{r_f}\left(\ln\frac{\sqrt{2r_iS+r^2}}{r}\right)^n dr + p_s(r_f-r_e)\right.$$

$$\left. - C\left(\frac{2}{\sqrt{3}}\right)^{n+1}\int_{r_e}^{r_f}\int_r^a\frac{1}{r}\left(\ln\frac{\sqrt{2r_iS+r^2}}{r}\right)^n dr\cdot dr\right\} \ . \tag{19}$$

In the same manner, substituting the sum of σ_{riF}, σ_G and σ_H for σ_{ri} in Eq. (3), the equation of punch pressure p_P, in which the frictional effect is considered, can be expressed as:

$$p_P = \frac{2r_i t}{r_p^2}\left\{C\left(\frac{2}{\sqrt{3}}\right)^{n+1}\int_{r_i}^{a}\frac{1}{r}\left(\ln\frac{\sqrt{2r_iS+r^2}}{r}\right)^n dr - p_S\right\}$$
$$+\frac{r_i t^2 C}{2\rho r_p^2}\left\{\left(\frac{2}{\sqrt{3}}\ln\frac{\sqrt{2r_iS+r_e^2}}{r_e}\right)^n+\left(\frac{2}{\sqrt{3}}\ln\sqrt{\frac{2S}{r_i}+1}\right)^n\right\}$$
$$+\frac{4r_i\mu}{r_p^2}\left\{\frac{C}{\sqrt{3}}\left(\frac{2}{\sqrt{3}}\right)^n\int_{r_e}^{r_f}\left(\ln\frac{\sqrt{2r_iS+r^2}}{r}\right)^n dr + p_S(r_f-r_e)\right.$$
$$\left.-C\left(\frac{2}{\sqrt{3}}\right)^{n+1}\int_{r_e}^{r_f}\int_{r}^{a}\frac{1}{r}\left(\ln\frac{\sqrt{2r_iS+r^2}}{r}\right)^n dr\cdot dr\right\}. \qquad (20)$$

In Eqs. (19) and (20), both of the drawing force F and punch pressure p_P are expressed as the function of drawing depth S and lateral fluid pressure p_S. In Eq. (19), however, p_S is included only in frictional term, so it does not have much effect on F.

3. Calculation of Drawing Force

By using the theoretical equations obtained in the preceding chapter, the theoretical values of drawing force and punch pressure were calculated for the working condition shown in the previous paper[1]. And they were compared with the experimental value of drawing force[2] and that of punch pressure[1], respectively.

Table 1 shows the factors to calculate these theoretical values, and the calculation factors are based on the experimental conditions[1] for aluminum sheets A1050P-0. The value of coefficient of friction μ shown in this table was obtained from the friction test, and it was almost the same as the value obtained from compression test for aluminum cylinder under tallow lubrication carried out by Tanaka et al.[3]

Table 1 Calculation factors

Diameter of blank	$2a_0$ /mm	60.0
Thickness of blank	t /mm	0.8, 1.5
Work hardening factor	C /MPa	150 (t = 0.8) 145 (t = 1.5)
Work hardening exponent	n	0.28 (t = 0.8) 0.27 (t = 1.5)
Coefficient of friction	μ	0.02
Punch diameter	$2r_p$/mm	15.0
Die throat diameter	$2r_d$/mm	16.9 (t = 0.8) 18.7 (t = 1.5)
Die profile radius	ρ_d/mm	2.5
Diameter of die opening	$2r_e$/mm	21.9 (t = 0.8) 23.7 (t = 1.5)
Diameter of protrusion of hold-down cylinder	$2r_f$/mm	26.0 (t = 0.8) 28.0 (t = 1.5)

Figure 2 shows the theoretical curves of $F-S$ for 0.8 mm and 1.5 mm thick sheets under set lateral fluid pressure $p_s = 140$ MPa (1400 kgf/cm^2), and the marks of (O) and (Δ) indicate the experimental values of F shown in the previous paper[2]. In this figure, two chain lines show the drawing forces F_s due to the set lateral fluid pressure p_s for both sheets. For depth of drawing S below 15 mm, the theoretical results agree very well with the experimental values. But for S above 15 mm, the theoretical results deviate gradually from the experimental values, because the formation of ears caused by anisotropy of sheet is unconsidered in this theoretical equation in which axisymmetric deformation is assumed.

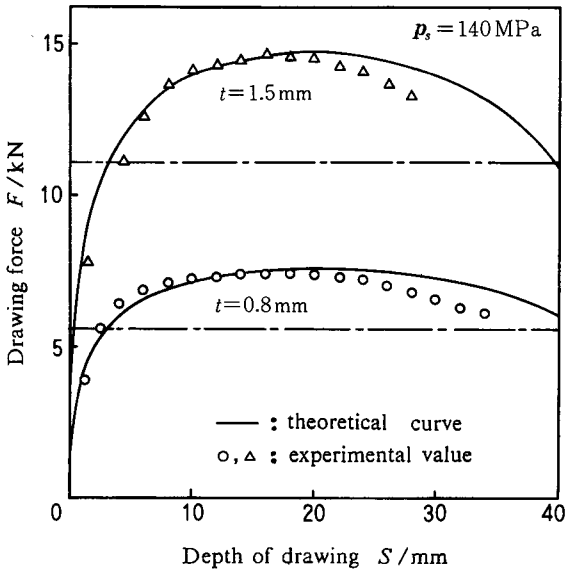

Fig. 2 $F-S$ diagram.

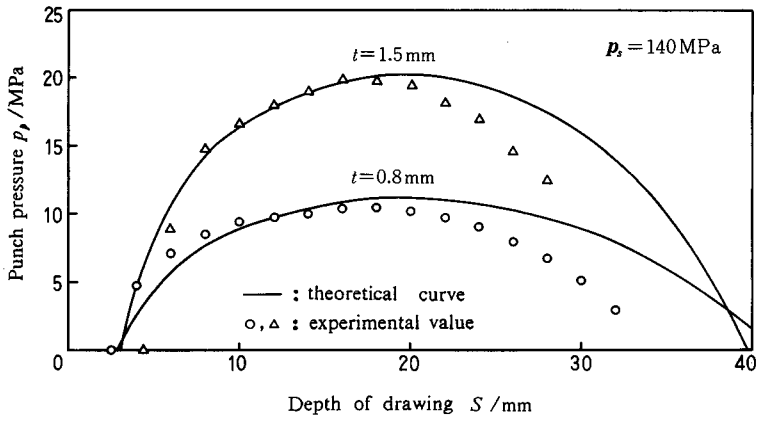

Fig. 3 $p_p - S$ diagram

Figure 3 shows the theoretical curves of $p_P - S$ for 0.8 mm and 1.5 mm thick sheets under $\boldsymbol{P}_s$ = 140 MPa, and the marks of (○) and (△) in this figure indicate the experimental values of p_P shown in the previous paper[1]. For S below 15mm, the theoretical results of p_P agree well with experimental values. But for S above 15 mm, the theoretical results deviate considerably from the experimental values, and the deviation is remarkable than that shown in Fig.2. Because, these $p_P - S$ curves correspond to $F_P - S$ curves which are equivalent only to the upper parts of $F - S$ curves divided by the chain lines shown in Fig. 2 as described in the previous paper[2].

The theoretical values of F and p_P were also compared with their experimental values for various set lateral fluid pressure $\boldsymbol{P}_s$ other than 140 MPa, and it was confirmed that their relations have the same tendency as those shown in Fig. 2 and Fig. 3.

4. Conclusion

In this study, the theoretical equations of the drawing force and punch pressure, in which bending and frictional effects were considered, were derived by the stress analysis based on the assumption of axisymmetric deformation and plane strain. And the good agreements between the theoretical values calculated by these equations and the experimental values were obtained for the drawing process except the last stage. Therefore, the drawing characteristics in this deep drawing, which is represented by the relation between the drawing depth, punch pressure, and lateral fluid pressure, may be estimated theoretically for different working conditions by use of these equations.

Reference

1) K. Asakura, N. Kobayashi, T. Hanamoto and M. Kohzu, Bull. Univ. Osaka Prefecture, 31A, 171 (1982).
2) K. Asakura, N. Kobayashi and M. Kohzu, ibid., 32A, 147 (1983).
3) E. Tanaka, S. Semoto, Y. Suzuki and S. Watanabe, J. Japan Soc. Tech. Plasticity, 6, 148 (1965).